

Single-crystal structures of cucurbiturils-based supramolecular host-guest complexes for bioimaging

Hui Liu,^a Min Lin,^a Yu Cui,^a Weijin Gan,^a Jing Sun,^{*c} Bo Li,^{*b} and Yingjie Zhao^{*a}

^a College of Polymer Science and Engineering, Qingdao University of Science and Technology, Qingdao 266042, P. R. China.

^b Department of Cardiology, Zibo Central Hospital, Shandong University Zibo, 255000, P. R. China.

^c State Key Laboratory of Supramolecular Structure and Materials, College of Chemistry, Jilin University, Changchun 130012, P. R. China

E-mail: jingsun@qust.edu.cn, libosubmit@163.com, yz@qust.edu.cn

Supporting Information

Table of Contents

1. Supporting Methods

1.1 General materials and methods	S3
1.2 Synthesis	S5
1.3 ¹ H NMR (COSY, NOESY) spectra of 1 _CB[7] and 1 _CB[8]	S6
1.4 The single-crystal data of 1 _CB[7] and 1 _CB[8]	S6
1.5 Cell culture and staining	S6
1.6 Cytotoxicity study	S7
1.7 References	S8

2. Supporting Figures and Legends

Figure S1: Synthetic scheme	S9
Figure S2: Full spectra of ¹ H NMR titration experiment	S9
Figure S3: 2D NMR spectrum (600 MHz) of 1 _CB[7] and 1 _CB[8]	S11
Figure S4: ¹ H NMR of 1 _CB[7] and 1 _CB[8] at different concentrations	S10
Figure S5: UV-vis spectra of 1 _CB[7] and 1 _CB[8] at different concentrations	S10

Figure S6: ESI-mass spectrum of the complex of 1 _CB[8]	S12
Figure S7: ITC titration data and fitting curves	S12
Figure S8-9: Job's plot of 1 _CB[7] and 1 _CB[8]	S13
Figure S10: Time-dependent fluorescence decay spectra of 1 _CB[7] and 1 _CB[8]	S14
Figure S11: Absorption and fluorescence spectra	S14
Figure S12: CLSM pictures of HeLa cells treated with 1	S15
Figure S13: DLS profiles of 1 _CB[7] solution and 1 _CB[8] solution	S15
Figure S14: Cytotoxicity study of 1 _CB[7] and 1 _CB[8]	S16
Figure S15-18: ¹ H NMR and ¹³ C NMR spectra of the obtained compounds	S16

1. Supplementary Methods

1.1 General Materials and Methods

Reagents for synthesis were purchased commercially and used without further purification. Trans-2-[3-(4-tert-butylphenyl)-2-methyl-2-propenylidene] malononitrile (DCTB) and tris(4-bromophenyl)amine were purchased from Adamas. 4',6-Diamidino-2-phenylindole (DAPI) and Lambda DNA (λ DNA) (48502 base pairs) were purchased from ThermoFisher Scientific. Cucurbit[7]uril (CB[7]) and Cucurbit[8]uril (CB[8]) were purchased from Sigma. Unless otherwise specified, all aqueous solutions were prepared with Milli-Q water.

All reactions were carried out under nitrogen condition unless otherwise noted. ^1H and ^{13}C NMR spectra were performed on 400 MHz spectrometers (Bruker AVANCE NEO 400 Ascend) in the indicated solvents at room temperature. Chemical shifts were reported in δ (ppm) relative to TMS ($\delta=0$). Two-dimensional nuclear magnetic resonance spectroscopy (2D NMR) was recorded on Agilent NMR Spectrometer (600-54-ASC) with deuterium oxide (D_2O) as solvent. Unless otherwise indicated, column chromatography was carried out on silica gel (200-300 mesh). Thin-layer chromatography (TLC) analysis was performed on precoated silica gel plates (0.2 mm thick). Matrix-Assisted Laser Desorption/Ionization Time of Flight Mass Spectrometry (MALDI-TOF MS) analysis was performed on a Bruker Microflex-LRF mass spectrometer in positive ion, reflection mode. Electron spin-resonance spectroscopy (ESR) measurements were performed on a Bruker A300 apparatus, with 9853 MHz

microwave frequency and 20.16 mW power. Scanning electron microscopy (SEM) images were collected using a scanning electron microscope (JEOL, JSM-7500F) at an accelerating voltage of 5.0 kV. The UV-vis absorbance was measured by UV spectrometer (HITACHI, 3900). Fluorescence spectra were recorded on a fluorescence spectrometer (HITACHI, F-2700). Confocal laser scanning microscope (CLSM) images were recorded on Nikon C2 plus (NIKON CORPORATION, Japan). Mass spectra (ESI) were obtained on Bruker impact II time-of-flight mass spectrometer. Isothermal titration calorimetry (ITC) experiments were carried out on a PEAQ-ITC microcalorimetric system with a nickel alloy sample cell of 200 μ L at room temperature. All the sample solutions for titration were prepared with Milli-Q water. Dynamic light scattering (DLS) was performed on Malvern Zetasizer Nano ZS90. Time-dependent fluorescence decay spectra were measured at room temperature using FLS 1000 spectrometer (Edinburgh Instruments, UK). The data was fit with the exponential reconvolution function and the non-linear least square method. The absolute fluorescence quantum yield was determined on the C11347-11 absolute quantum yield spectrometer (HAMAMATSU, Japan).

Abbreviations. Dichloromethane (DCM), trichloromethane (CHCl_3), N,N-dimethylformamide (DMF), methanol (MeOH), dimethylsulfoxide (DMSO), trans-dichlorobis(triphenyl-phosphine)palladium(II) ($\text{PdCl}_2(\text{PPh}_3)_2$), methyl iodide (CH_3I), Cucurbit[7]uril (CB[7]), Cucurbit[8]uril (CB[8]), thin-layer chromatography (TLC), Matrix-Assisted Laser Desorption/Ionization Time of Flight Mass Spectrometry

(MALDI-TOF MS), Dynamic Light Scattering (DLS), Scanning electron microscopy (SEM).

1.2 Synthesis

Compound 2. To a stirred solution of tris(4-bromophenyl)amine (0.443 g, 0.92 mmol) in DMF (20 mL) was added 4-vinylpyridine (0.483 g, 4.6 mmol), PdCl₂(PPh₃)₂ (0.064 g, 0.092 mmol), and potassium carbonate (0.758 g, 5.49 mmol). The reaction solution was refluxed overnight. The reaction solution was cooled down and poured over 150 mL ice water. The precipitate was collected by filtration, washed with H₂O. Silica gel column chromatography of the residue (DCM/MeOH, 20:1) gave pure **2** (0.357 g, 70% yield) as an orange solid. ¹H NMR (400 MHz, CDCl₃): 8.57 (d, *J* = 6.1 Hz, 6H), 7.47 (d, *J* = 8.6 Hz, 6H), 7.36 (d, *J* = 6.2 Hz, 6H), 7.28 (d, *J* = 13.2 Hz, 3H), 7.14 (d, *J* = 8.6 Hz, 6H), 6.94 (d, *J* = 16.3 Hz, 3H). ¹³C NMR (101 MHz, CDCl₃): 150.07, 147.31, 144.84, 132.42, 131.34, 128.19, 124.81, 124.38, 120.71. MS (MALDI-TOF): 555 [M+H]⁺.

Compound 1. A mixture of **2** (0.055 g, 0.1 mmol), CH₃I (0.709 g, 5 mmol), CHCl₃/MeOH (6 mL, 1/5 by vol.) was stirred at 25 °C for 12 h. The mixture was cooled down and the precipitate was collected by centrifugation, washed with DCM for several times to afford **1** (0.066 g, 91% yield) as a red solid. ¹H NMR (400 MHz, DMSO-*d*₆): 8.84 (d, *J* = 6.9 Hz, 6H), 8.21 (d, *J* = 6.9 Hz, 6H), 8.03 (d, *J* = 16.3 Hz, 3H), 7.77 (d, *J* = 8.7 Hz, 1H), 7.45 (d, *J* = 16.2 Hz, 3H), 7.20 (d, *J* = 8.7 Hz, 6H), 4.25 (s, 9H). ¹³C NMR (101 MHz, DMSO-*d*₆): 153.02, 148.20, 145.47, 140.40, 131.26, 130.32, 124.85,

123.72, 122.57, 47.33. MS (MALDI-TOF): 600 [M-3I]³⁺, 727 [M-2I]²⁺, 854 [M-I]⁺.

1.3. ¹H NMR (COSY, NOESY) spectra of 1_CB[7] and 1_CB[8]

2D correlation spectroscopy (COSY) spectra are used to identify each proton (Figure S4c, d). The 2D nuclear overhauser spectroscopy (NOESY) spectrum of 1_CB[8] revealed obvious NOE connections between H^d and H^e, H^e and H^f. No relationships between H^a and H^f, H^b and H^d were observed, indicating the formation of a dimer adopting head-to-head arrangement of the 4-styrylpyridinium arms located inside the cavity of CB[8] (Figure S4f).

1.4. The single-crystal data of 1_CB[7] and 1_CB[8]

Table S1. Crystal data and structure refinement.

CCDC	2059161	2036099
Identification code	1_CB[7]	1_CB[8]
Empirical formula	C ₁₆₈ H ₁₆₅ I ₃ N ₈₈ O ₄₂	C ₄₃₄ H ₄₇₆ I ₁₂ N ₂₀₂ O ₁₄₂
Formula weight	4469.48	12316.94
Temperature/K	169.97(13)	169.99(10)
Crystal system	hexagonal	orthorhombic
Space group	P6 ₃ /m	C222 ₁
a/Å	29.8173(2)	33.5039(3)
b/Å	29.8173(2)	46.8236(4)
c/Å	18.0740(2)	85.2422(8)
α/°	90	90
β/°	90	90
γ/°	120	90
Volume/Å ³	13916.2(2)	133726(2)
Z	2	8
ρ _{calc} /cm ³	1.067	1.224
F(000)	4568.0	50128.0
Crystal size/mm ³	0.28 × 0.12 × 0.08	0.245 × 0.231 × 0.112
Reflections collected	177826	247869
Independent reflections	9915 [R _{int} = 0.0524, R _{sigma} = 0.0130]	118717 [R _{int} = 0.0660, R _{sigma} = 0.0583]
R1 indices	0.1755	0.2014

1.5 Cell culture and staining^{1,2}

Hela cells were cultured in Dulbecco's modified eagle medium (DMEM) supplemented with 10% fetal bovine serum (FBS) and 1% P/S in an atmosphere of 5% CO₂ and 95%

air at 37°C for 24 hours. Then the culture supernatant was aspirated. The cells were fixed with paraformaldehyde in PBS (3%). The cells were co-stained with an aqueous solution of DAPI (10 µg/ml) and host-guest complexes (**1**_CB[7] or **1**_CB[8]) for 20 min. Afterward, the cells were extensively washed with PBS to remove the excess of the unbound dye. The slides were mounted and imaged by CLSM.

1.6 Cytotoxicity study³

The relative cytotoxicities of the host-guest complexes (**1**_CB[7] or **1**_CB[8]) were assessed using methyl thiazolyl tetrazolium (MTT) viability assay against HeLa cells. HeLa cells were cultured in DMEM medium containing with 10% FBS, 1% P/S. Then 100 µL of the suspension (2×10^5 cells per ml supplemented) were seeded in each well of a 96-well plate. The plate was then incubated in a humidified 5% CO₂ in air incubator at 37°C for 24 h. After aspirating original medium, the host-guest complexes in H-DMEM medium at different concentrations were added into each well of 96-well plate. And the plate was incubated under the same condition (5% CO₂ in air incubator, 37°C) for 24 h. Then 10 µL MTT solution (5 mg mL⁻¹ in PBS) was added to each well and the plate was incubated under the same condition (5% CO₂ in air incubator, 37°C) for 4 h. Next, the MTT solution and medium were removed and 150 µL DMSO was added to dissolve the formazan crystals. After 30 min, the optical absorbance at 490 nm was measured on a Tecan Sparkmicroplate reader. A nontoxic control experiment was carried out using the growth medium without the sample. A toxic control experiment was carried out using the growth medium with Tween 20 (30 µL Tween 20 per 100 µL growth medium). Cell viability (%) was analysed according to the following equation:

cell viability (%) = $(A_{\text{sample}} / A_{\text{control}}) \times 100\%$, where A_{sample} and A_{control} were the absorbances of the sample and control well, respectively. The measurements were performed in triplicate.

As shown in Figure S14, cell viability was still greater than 90% until the concentration of **1**_CB[7] and **1**_CB[8] reach 30 μM . These results suggest the good biocompatibility and low toxicity of the as-prepared complexes with the cells, making them promising materials for cell imaging applications.

1.7 References

- 1 X. Zhen, J. Zhang, J. Huang, C. Xie, Q. Miao and K. Pu, *Angew. Chem. Int. Ed.*, 2018, **57**, 7804-7808..
- 2 A. Clémence, S. Falk, L. Rémy, B. Guillaume, F. D. Céline, C. Fabrice, T. Patrick and T. F. Marie-Paule, *ChemBioChem*, 2007, **8**, 424-433.
- 3 X. Fu, Z. Li, M. Lin, J. Sun and Z. Li, *Eur. Polym. J.*, 2019, **119**, 281-288.

2. Supporting Figures and Legends

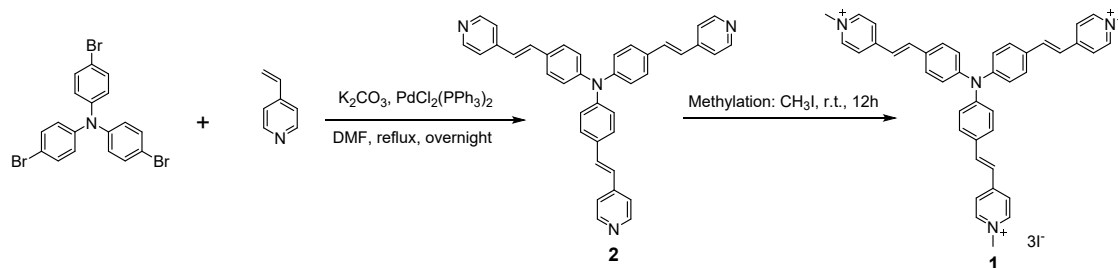


Figure S1. Synthetic scheme for the guest molecule **1**.

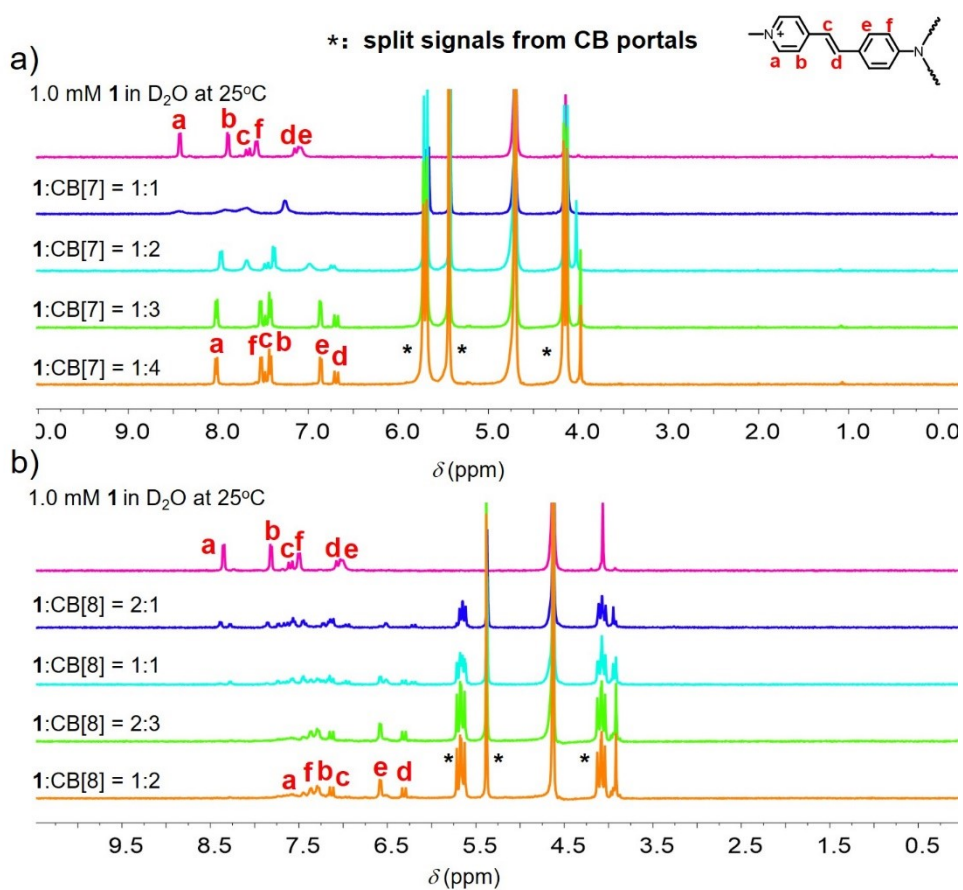


Figure S2. 1H NMR spectra: (a) **1** (1.0 mM) in D_2O in the presence of 0, 1.0, 2.0, 3.0, 4.0 equiv. of CB[7] at $25^\circ C$; (b) **1** (1.0 mM) in D_2O in the presence of 0, 0.5, 1.0, 1.5, 2.0 equiv. of CB[8] at $25^\circ C$.

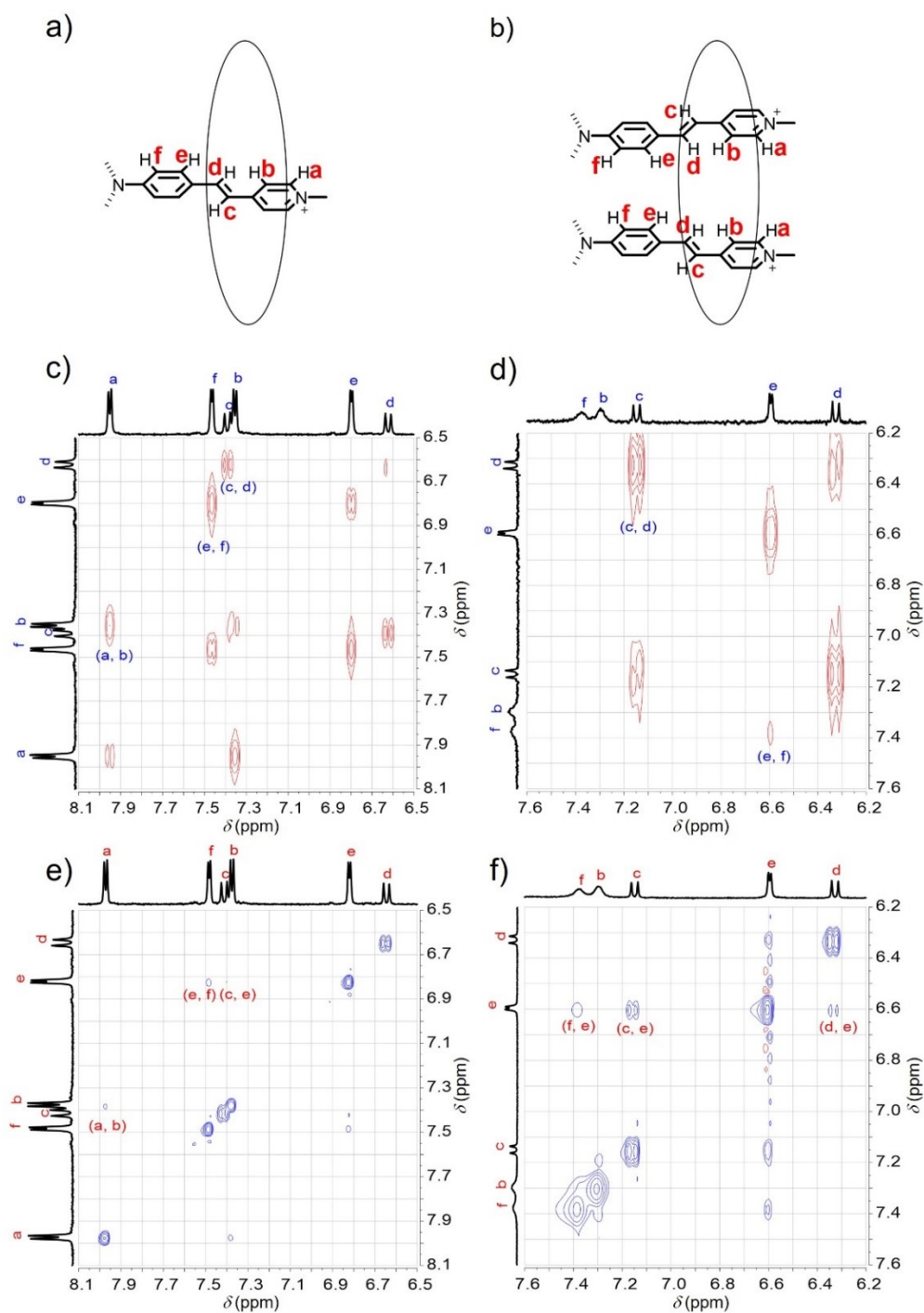


Figure S3. (a) Structural diagram of 1_{CB}[7], (c) correlation spectroscopy (COSY) and (e) nuclear overhauser effect spectroscopy (NOESY) spectrum of 1_{CB}[7] in D₂O at 25°C (The ratio between guests and CB[7] is 1:3; the concentration of 1_{CB}[7] is 1 mM). (b) Structural diagram of 1_{CB}[8], (d) COSY and (f) NOESY spectrum of 1_{CB}[8] in D₂O at 25°C (The ratio between guests and CB[8] is 2:3; the concentration of 1_{CB}[8] is 1 mM).

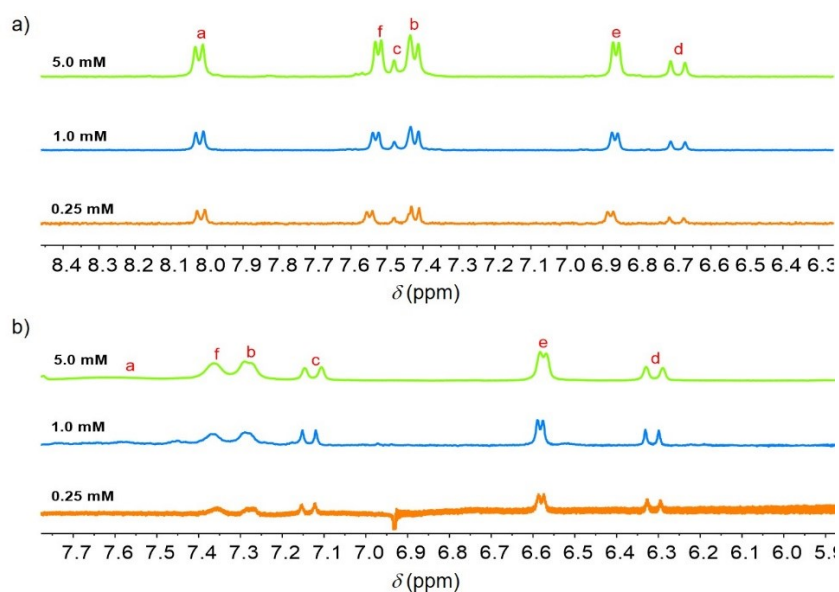


Figure S4. ^1H NMR spectra of (a) **1**_CB[7] and (b) **1**_CB[8] in D_2O at different concentrations.

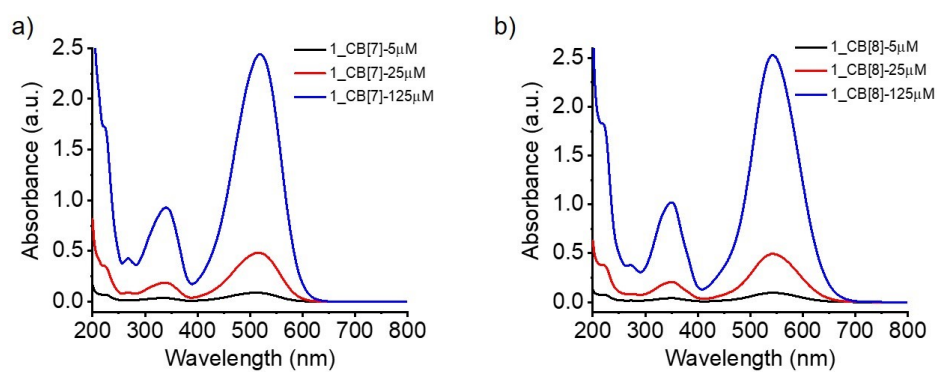


Figure S5. UV-vis spectra of (a) **1**_CB[7] and (b) **1**_CB[8] in H_2O at different concentrations (The ratios of guest to CB[7] and CB[8] were 1:3 and 2:3, respectively).

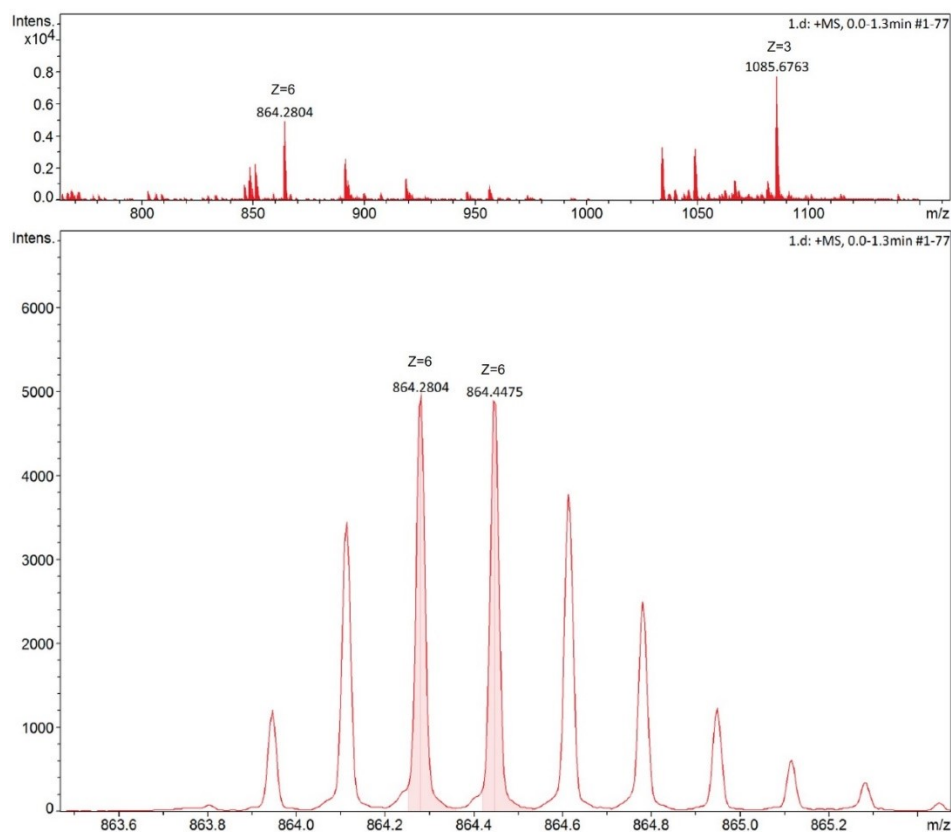


Figure S6. ESI-mass spectrum of the complex of **1**_CB[8].

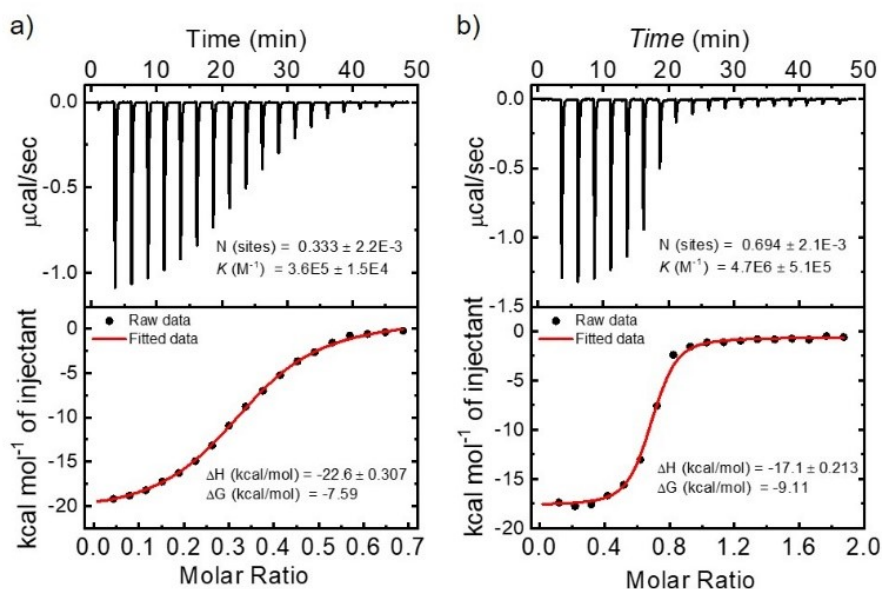


Figure S7. ITC titration data and fitting curves of (a) **1** (0.7 mM) titrated into CB[7] (0.1 mM) and (b) **1** (0.7 mM) titrated into CB[8] (0.05 mM).

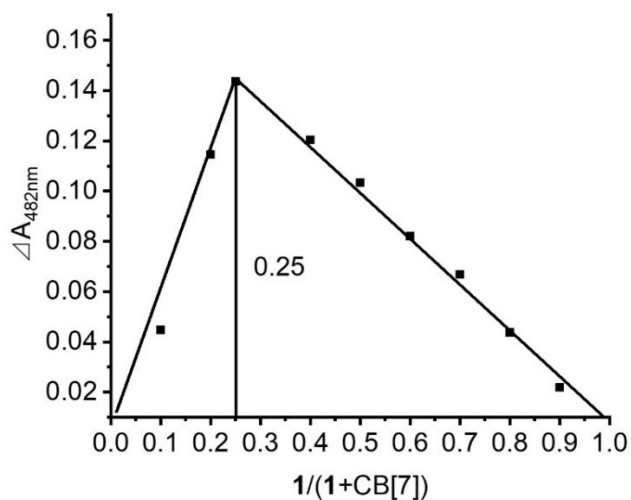


Figure S8. Job's plot obtained by recording the absorbance at 482 nm for the solution of **1** and CB[7] in H₂O at 25°C ($[1]_{tot} + [CB[7]]_{tot} = 2.0 \times 10^{-5}$ M), confirming the 1:3 stoichiometry of their complex.

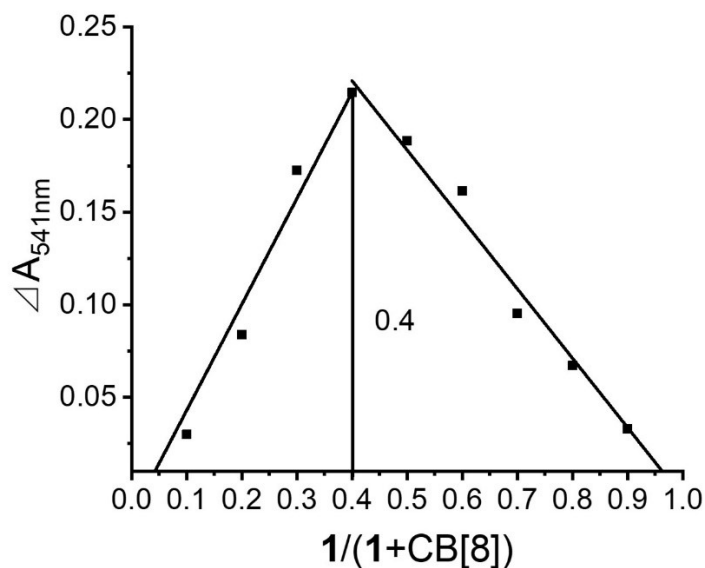


Figure S9. Job's plot obtained by recording the absorbance at 541 nm for the solution of **1** and CB[8] in H₂O at 25°C ($[1]_{tot} + [CB[8]]_{tot} = 2.0 \times 10^{-5}$ M), confirming the 2:3 stoichiometry of their complex.

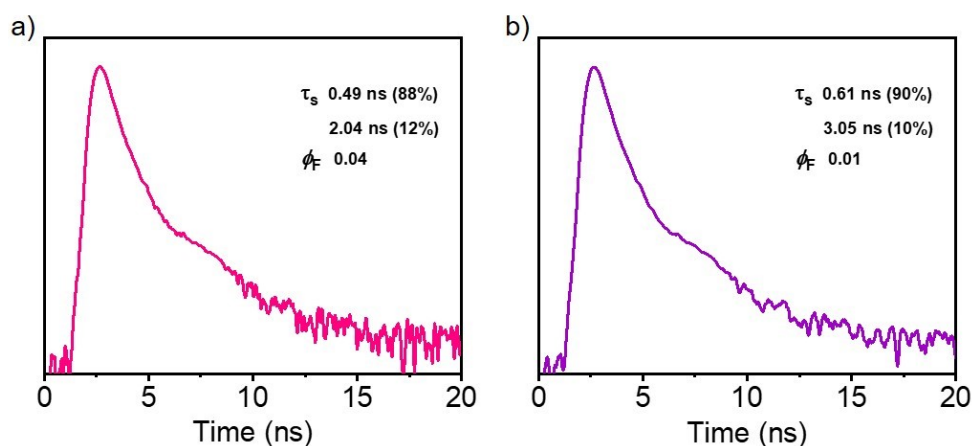


Figure S10. Time-dependent fluorescence decay spectra of (a) **1**_CB[7] and (b) **1**_CB[8] monitored upon excitation at 510 nm. All measurements were performed in water, with a guest concentration of 10 μ M.

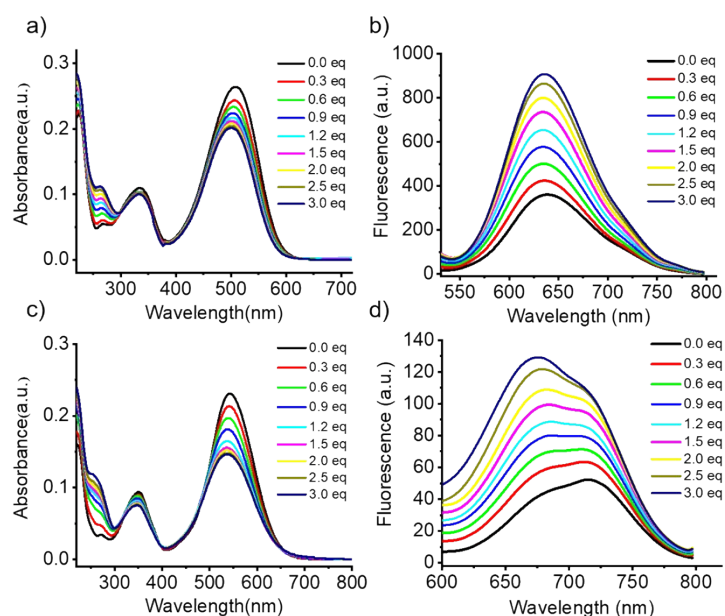


Figure S11. Absorption and fluorescence spectral changes of (a), (b) **1**_CB[7] (0.003 mM) and (c), (d) **1**_CB[8] (0.003 mM) upon gradual addition of λ DNA in water.

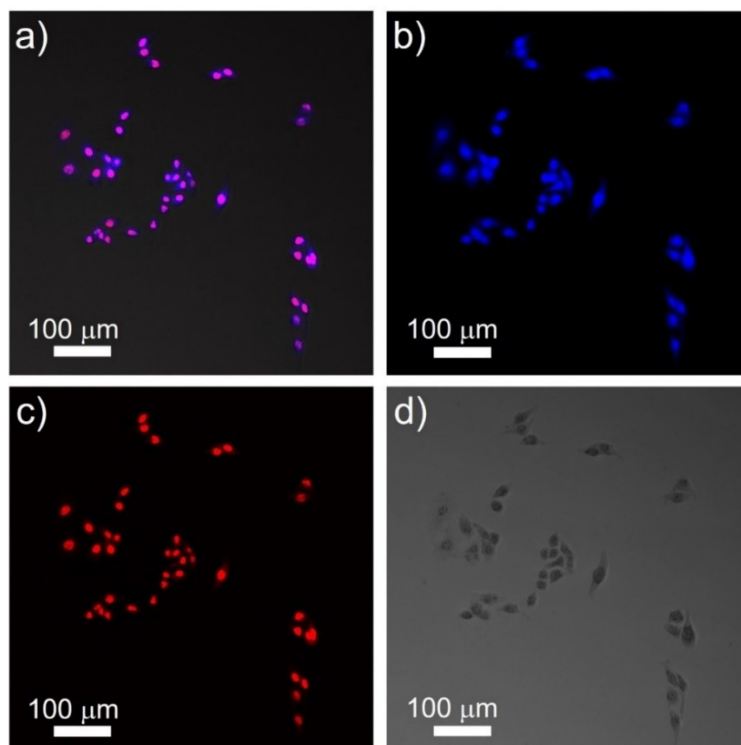


Figure S12. Laser scanning confocal microscopy pictures of HeLa cells treated with **1** (3 μM) and with DAPI (3 μM): (a) the merged picture, (b) fluorescence of DAPI, (c) fluorescence of **1** and (d) bright-field image.

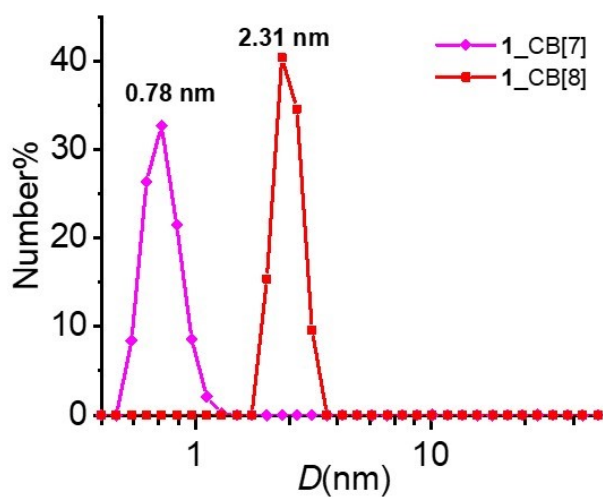


Figure S13. DLS profiles of **1**_CB[7] solution (0.01 mM, the ratio is 1:1) and **1**_CB[8] solution (0.01 mM, the ratio is 2:3) in water.

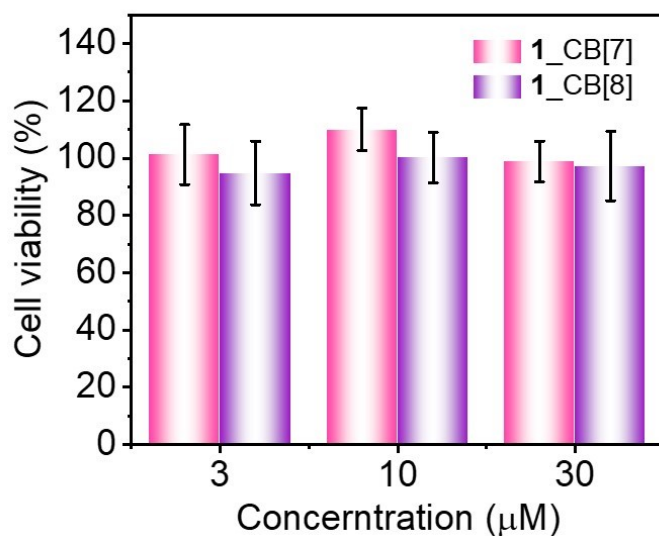


Figure S14. Cytotoxicity of **1**_CB[7] and **1**_CB[8] with different concentrations by MTT assay. The error bars are the standard deviations of four measurements.

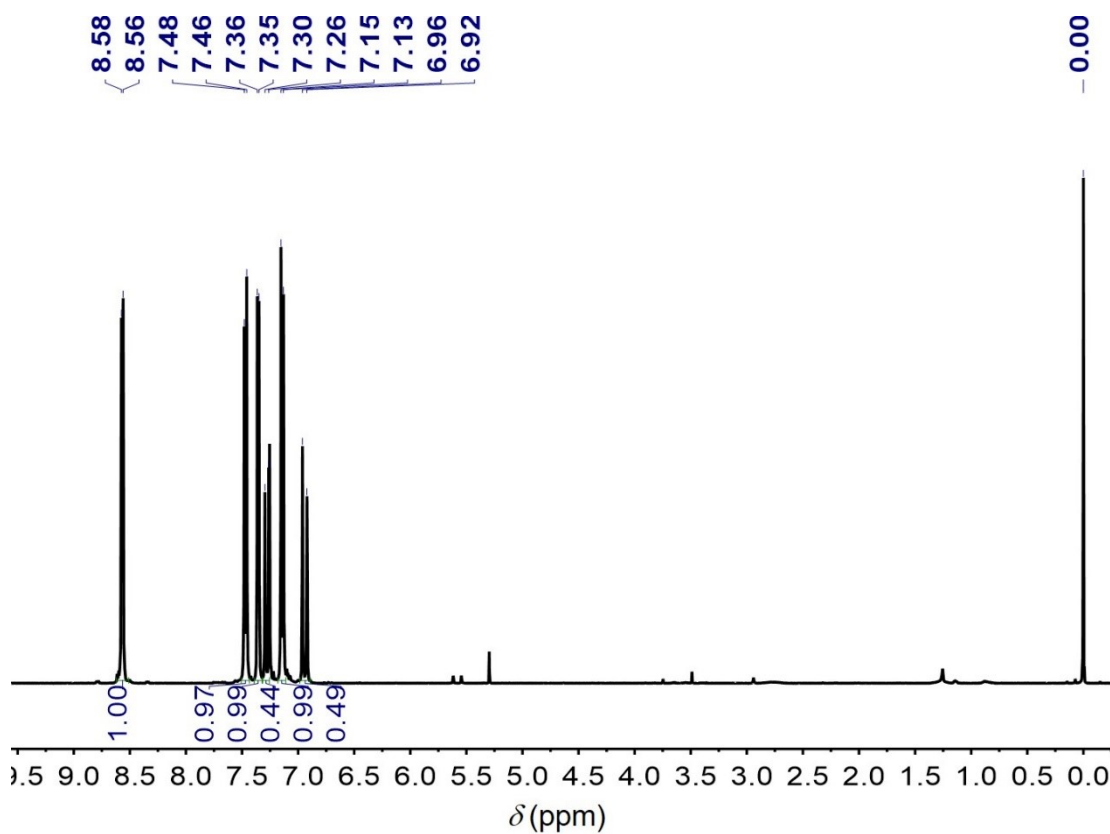


Figure S15. ^1H NMR (400 MHz) spectrum of compound **2** in CDCl_3 .

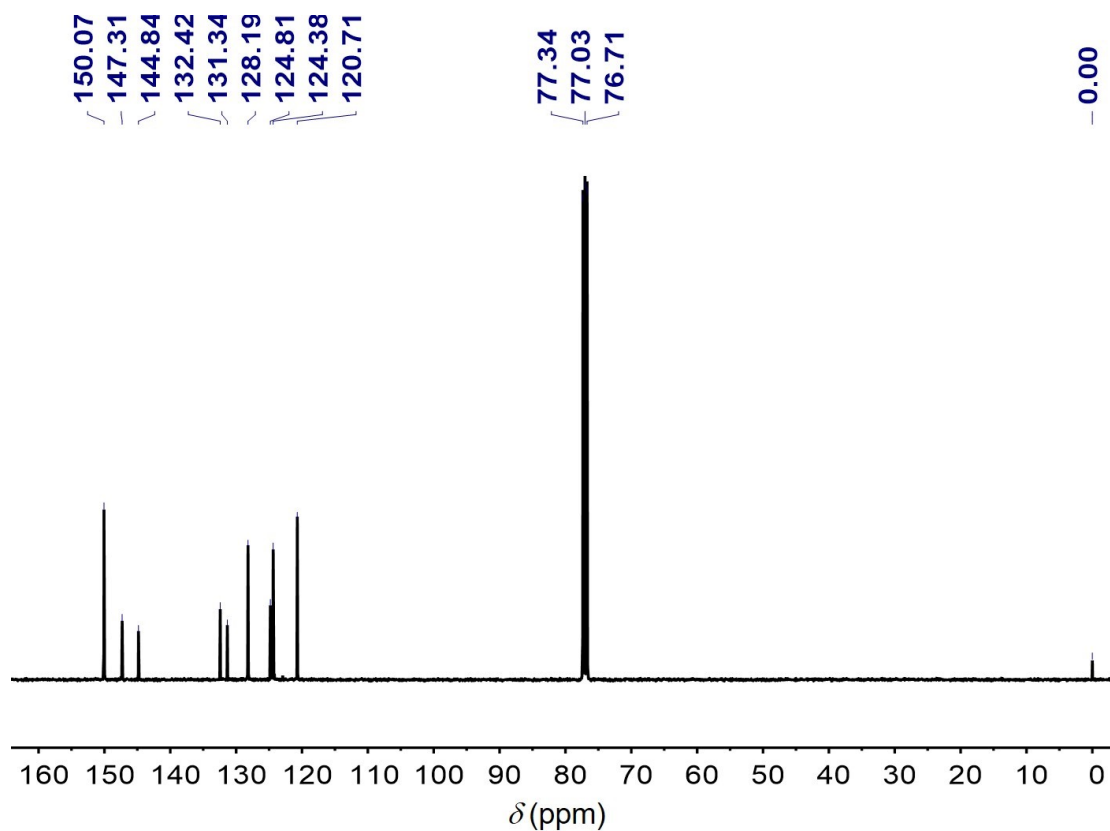


Figure S16. ^{13}C NMR (101 MHz) spectrum of compound **2** in CDCl_3 .

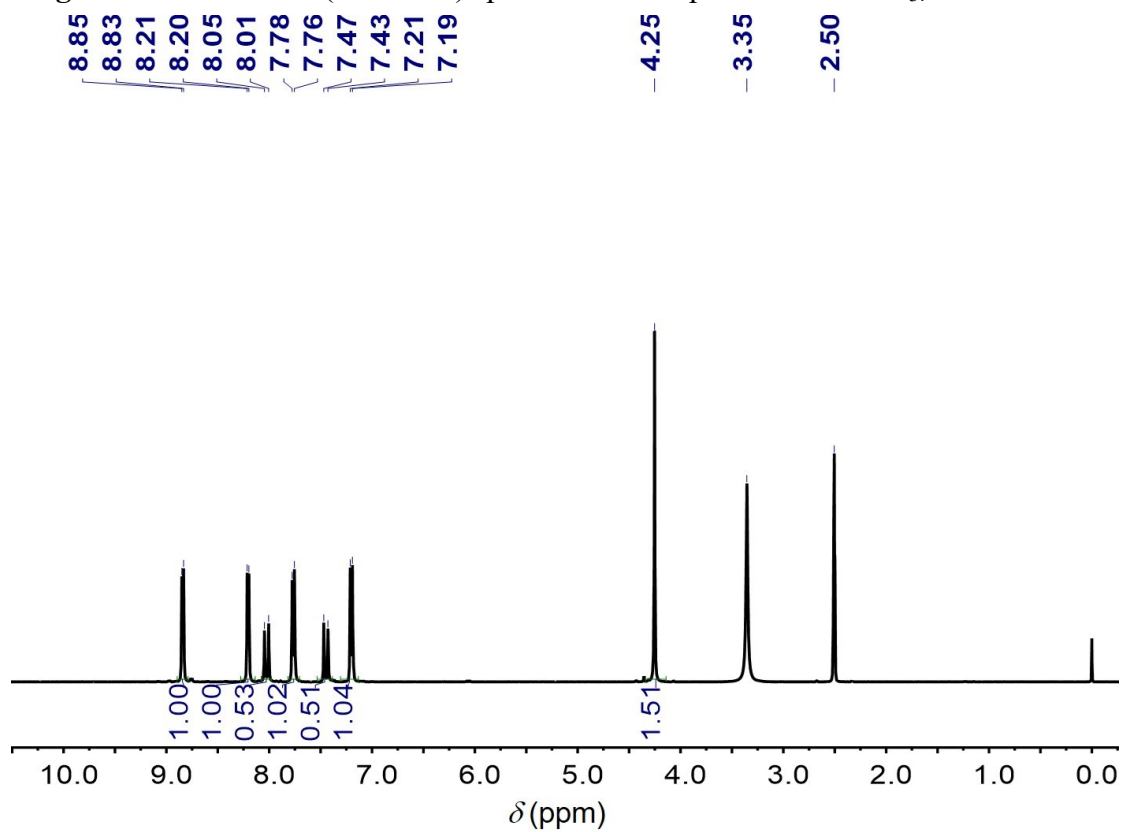


Figure S17. ^1H NMR (400 MHz) spectrum of compound **1** in $\text{DMSO}-d_6$.

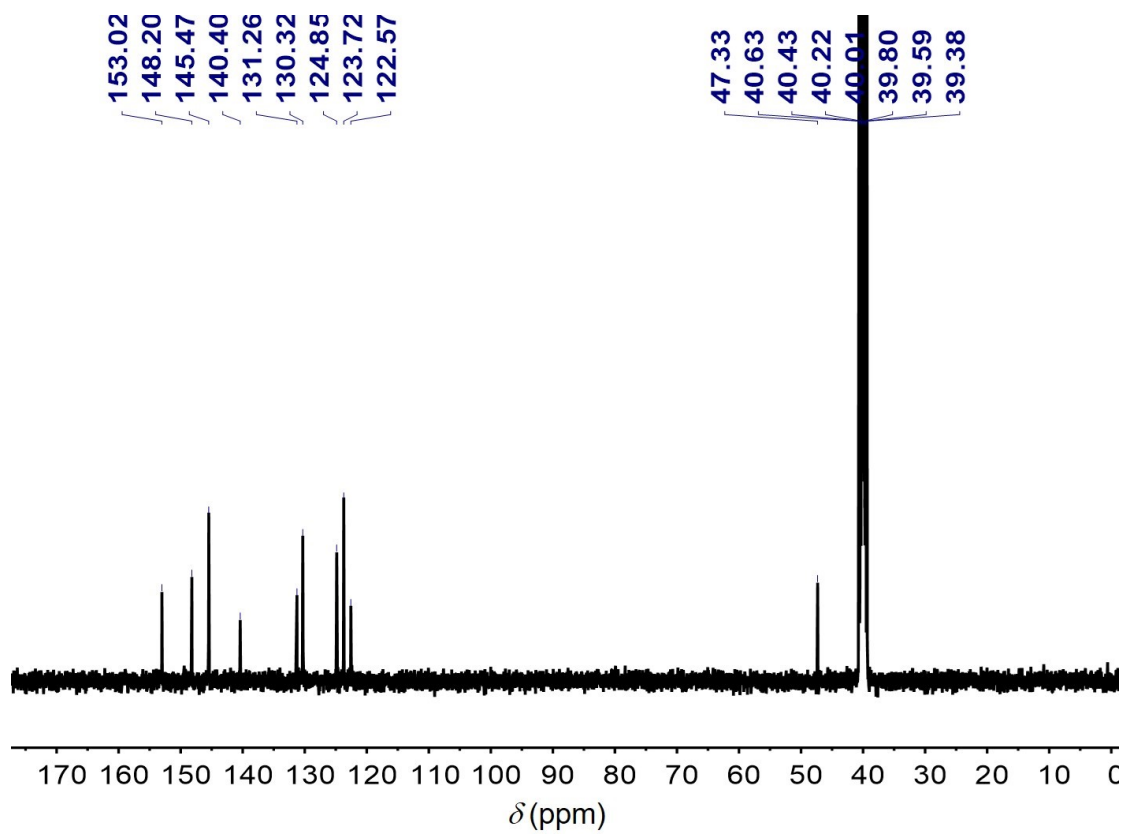


Figure S18. ¹³C NMR (101 MHz) spectrum of compound **1** in DMSO-*d*₆